Electronic Supporting Information

Reversible adsorption and storage of secondary explosives from water using a Tröger's base-functionalised polymer

Sankarasekaran Shanmugaraju,*[a] Deivasigamani Umadevi,[b] Aramballi J. Savyasachi,[a] Kevin Byrne,[b] Manuel Ruether,[a] Wolfgang Schmitt,[b] Graeme W. Watson,[b] and Thorfinnur Gunnlaugsson*[a]

[a]School of Chemistry and Trinity Biomedical Sciences Institute (TBSI), Trinity College Dublin, The University of Dublin, Dublin 2, Ireland.
[b]School of Chemistry and Centre for Research on Adaptive Nanostructures and Nanodevices (CRANN), Trinity College Dublin, The University of Dublin, Dublin 2, Ireland.

Table of Contents:

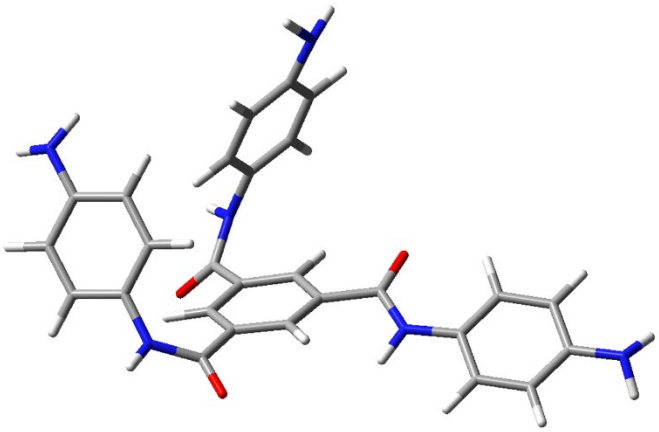

Fig. S1. Energy minimized structure of monomer **L**. Color code: gray, C; red, O; blue, N, white, H.

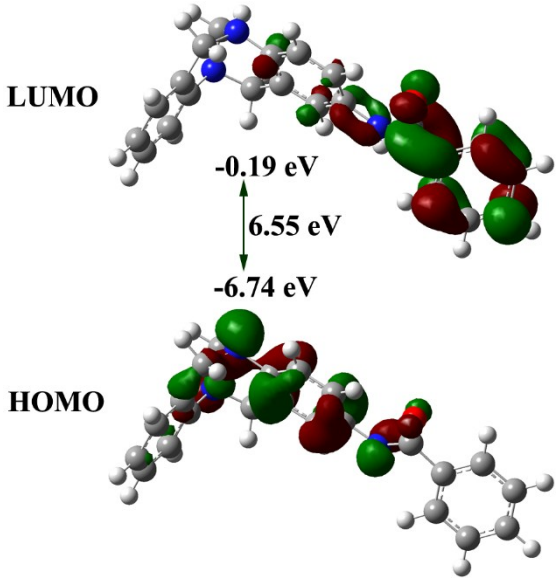

Fig. S2. Frontier molecular orbitals, with their corresponding energy values, for one monomer unit of **TB-COP**.

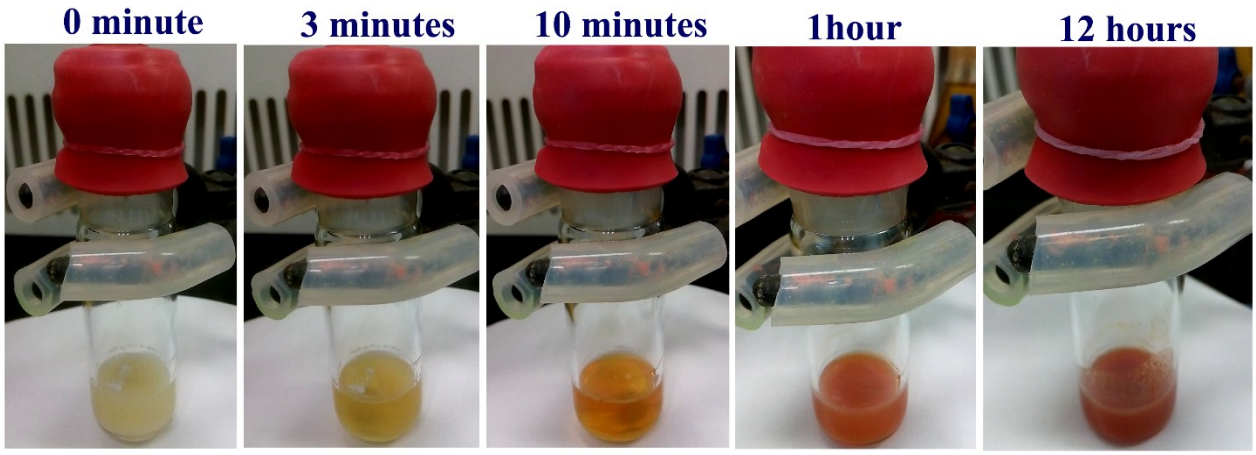

Fig. S3. Photographs of colour changes observed during the polymerization of monomer triamine (**L**) to Tröger's base polymer (**TB-COP**).

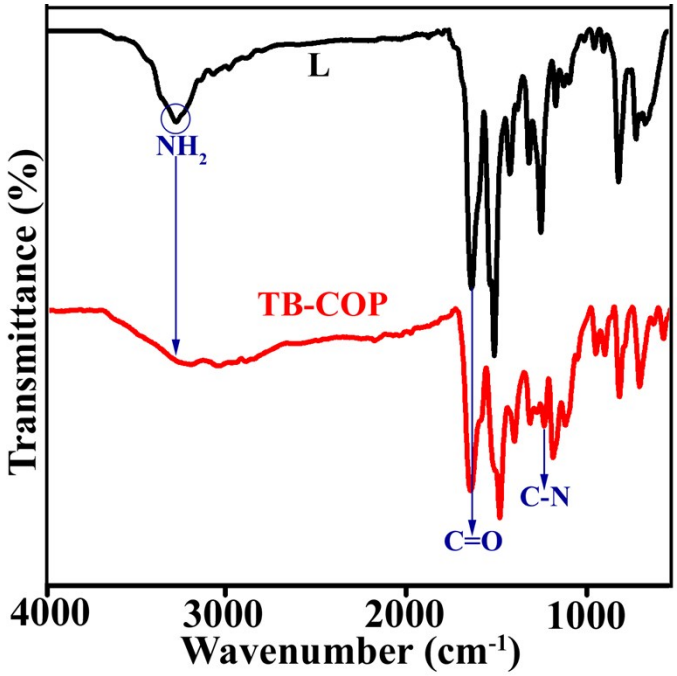

Fig. S4. FT-IR spectra of monomer triamine **L** (black) and polymer **TB-COP** (red).

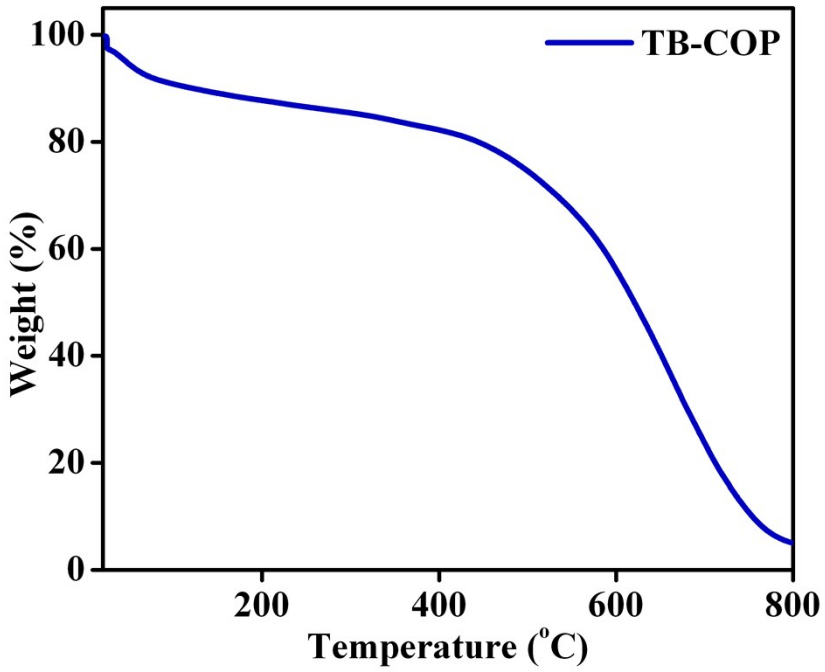

Fig. S5. Thermogravimetric analysis of as-synthesised **TB-COP** measured under N_2.

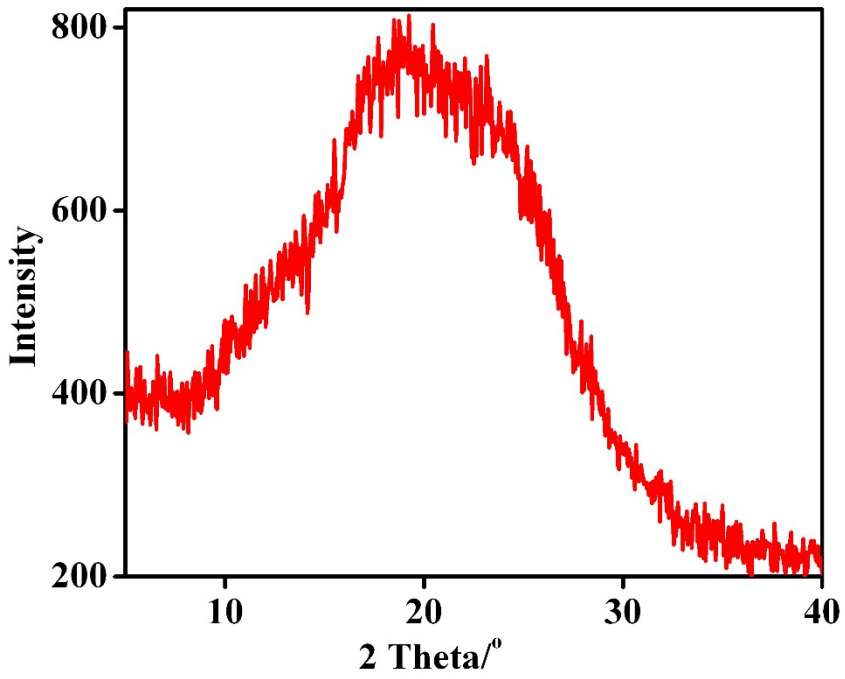

Fig. S6. X-ray powder diffraction pattern of as-synthesised **TB-COP**.

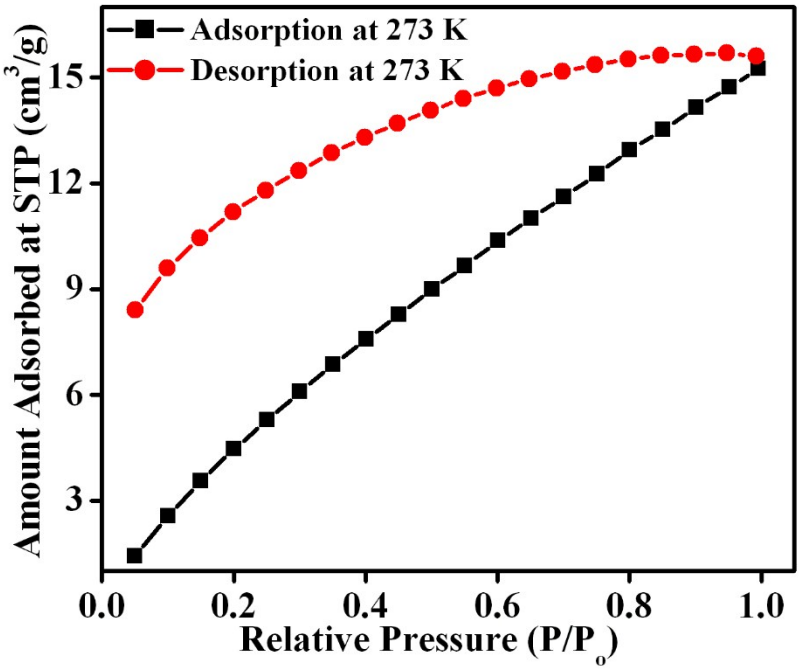

Fig. S7. The CO_2 adsorption-desorption isotherm measured at 273 K for **TB-COP**.

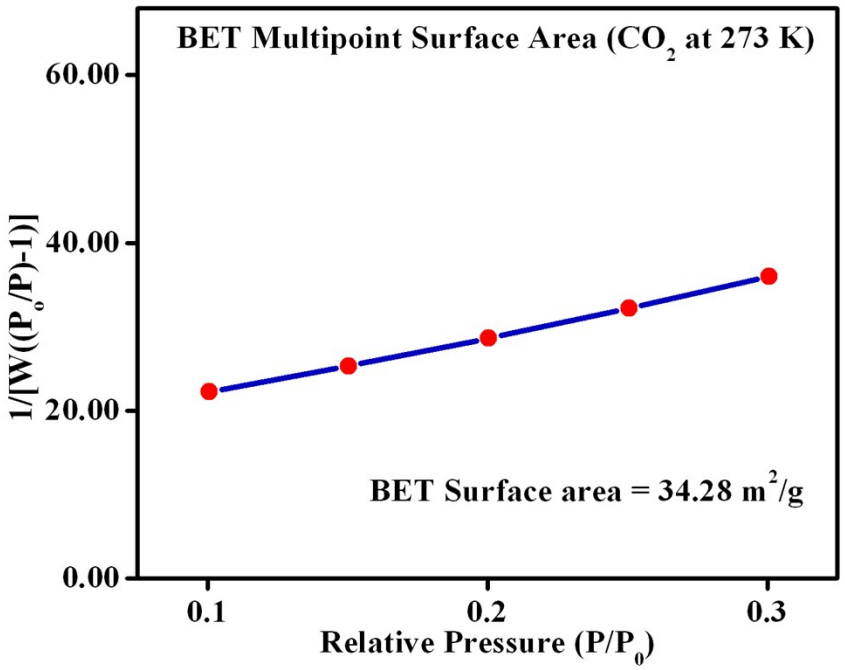

Fig. S8. BET linear plot and surface area of **TB-COP** calculated from CO_2 adsorption isotherm at 273 K.

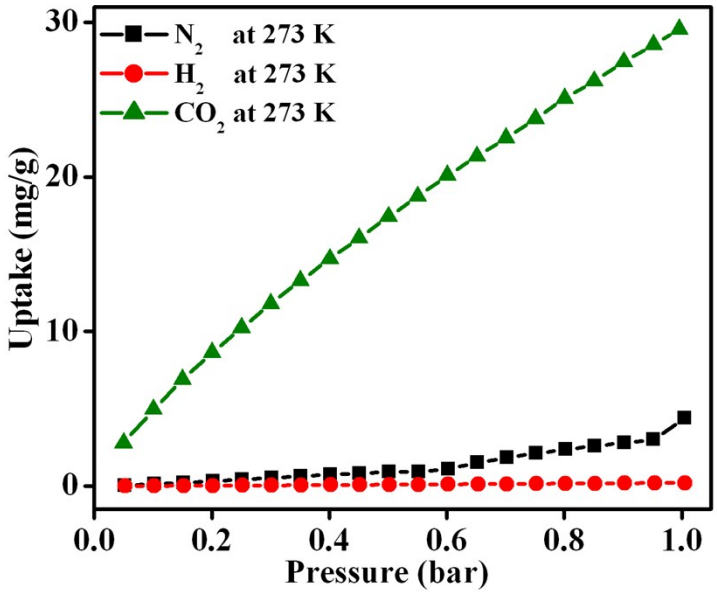

Fig. S9. The gas uptake capacitates of **TB-COP** for CO_2 over N_2 and H_2 at 273 K.

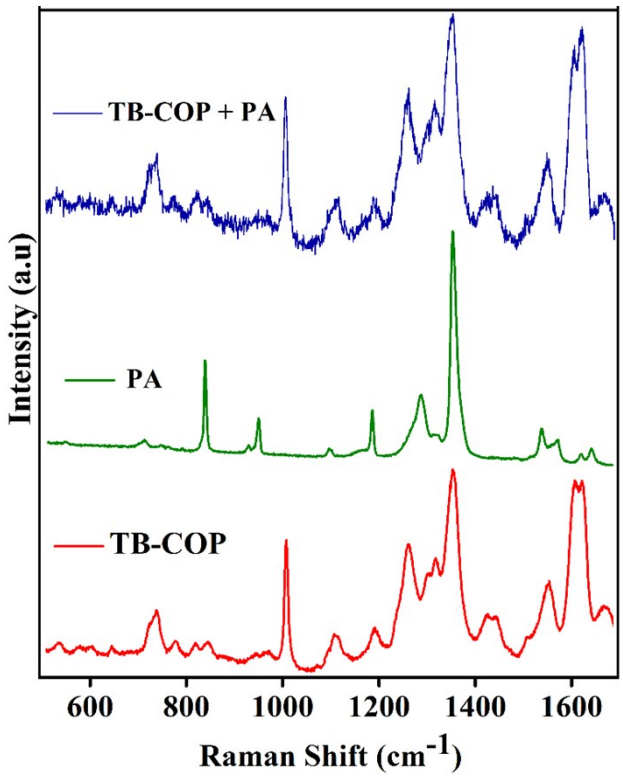

Fig. S10. Raman spectra of **TB-COP** and PA before and after the adsorption by **TB-COP**.

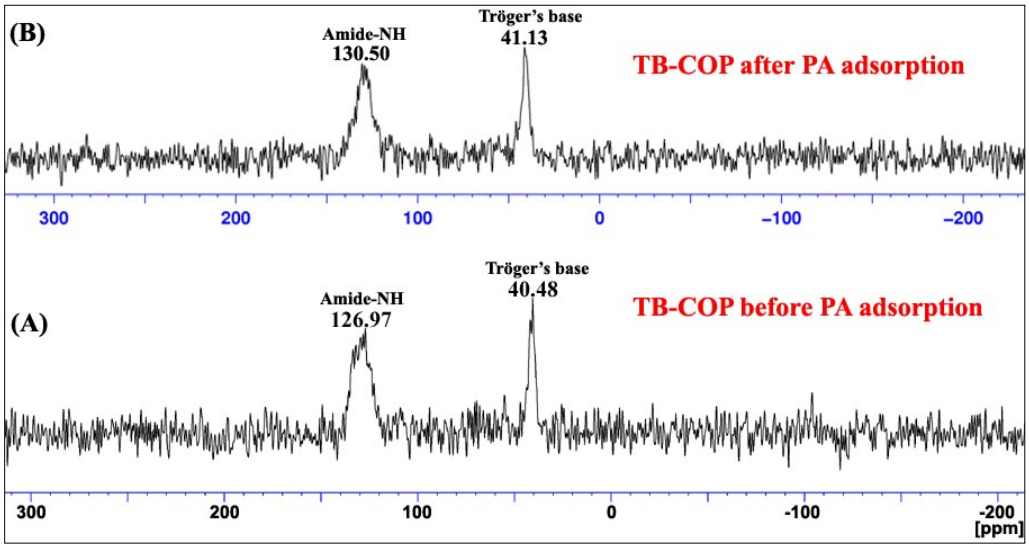

Fig. S11. The solid-state CP-MAS ^{15}N-NMR (400 MHz) spectrum **TB-COP** before (A) and after (B) adsorption of PA.

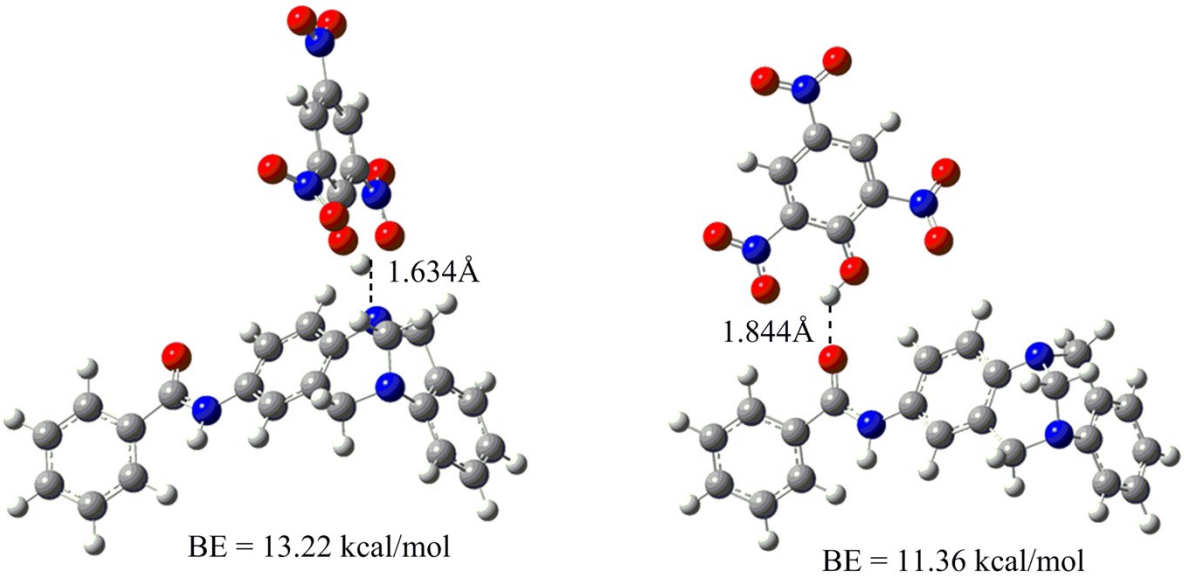

Fig. S12. Optimized structures, nearest intermolecular distances and the binding energy values of the two-possible mode of binding of PA with **TB-COP** (color codes: red = oxygen, blue = nitrogen, grey = carbon and white = hydrogen).

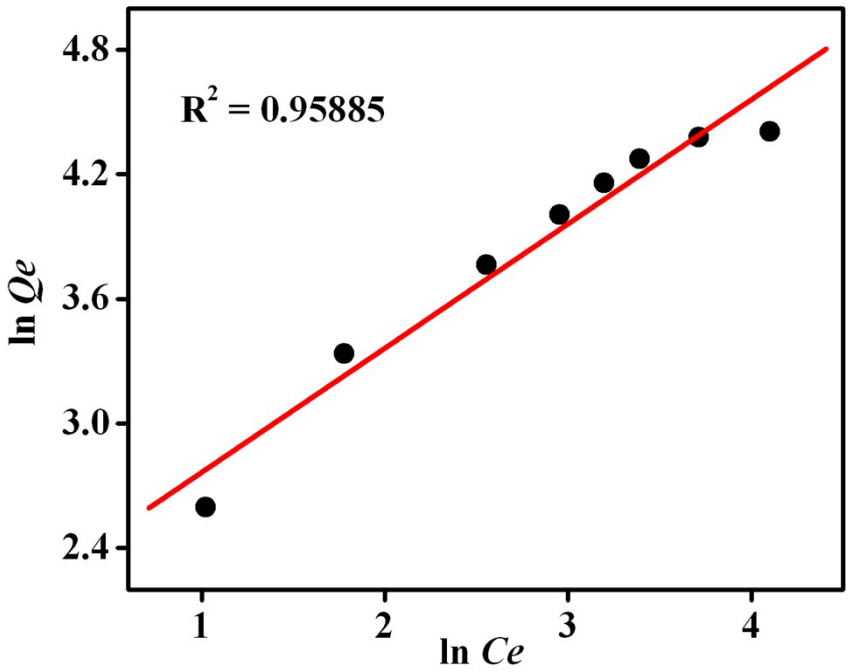

Fig. S13. Freundlich isotherm fitting for PA adsorption in **TB-COP.**

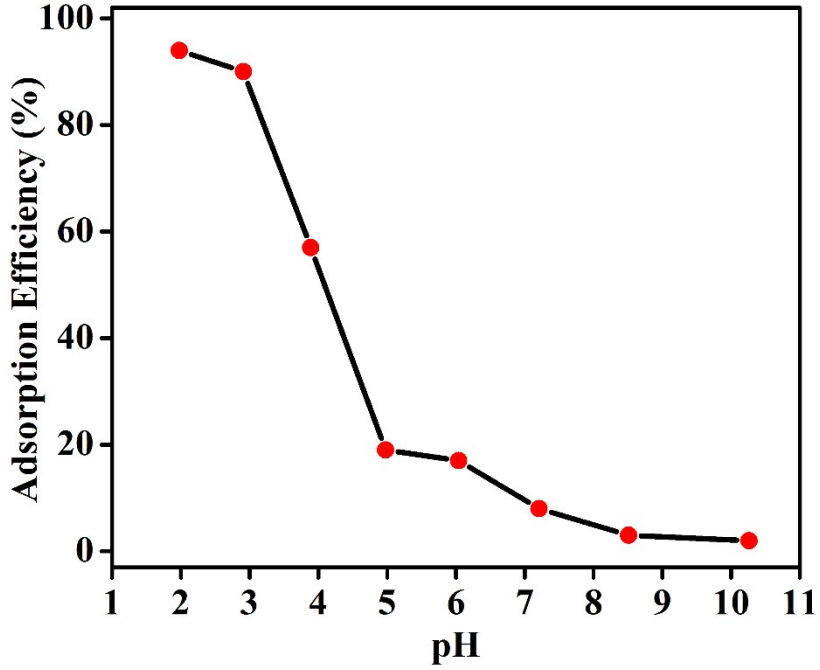

Fig. S14. The effect of pH on the extent of PA adsorption by **TB-COP** at 298 K.

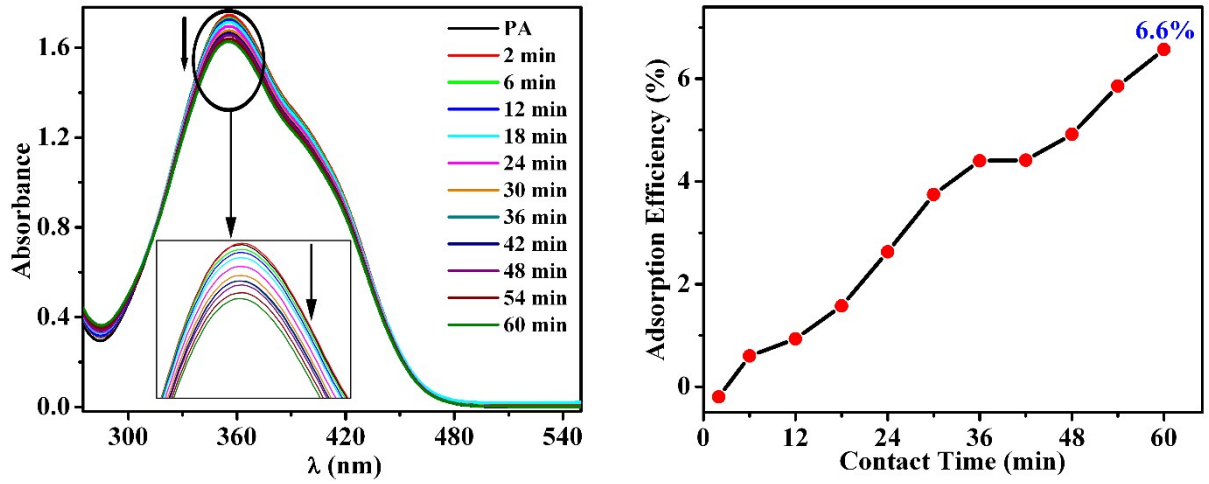

Fig. S15. Change in the absorption spectra (left) of the water solution of PA (0.5 mM) in the presence of **L** (3 mg) monitored at different time intervals (0→60 minutes) at 298 K and its corresponding adsorption efficiency plot (right).

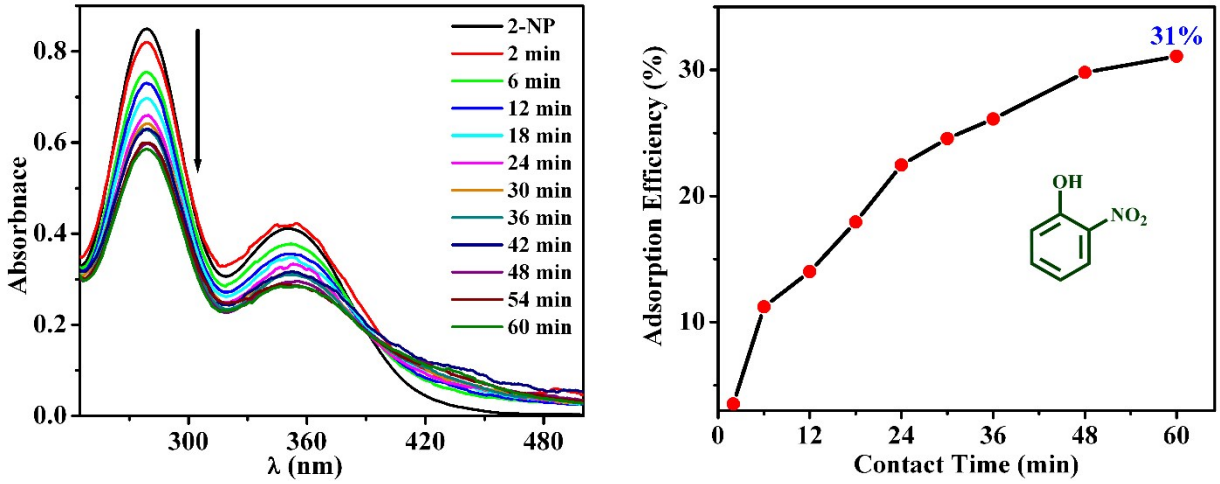

Fig. S16. Change in the absorption spectra of the water solution of 2-NP (0.5 mM) in the presence of **TB-COP** (3 mg) monitored at different time intervals (0→60 minutes) at 298 K and its corresponding adsorption efficiency plot (right).

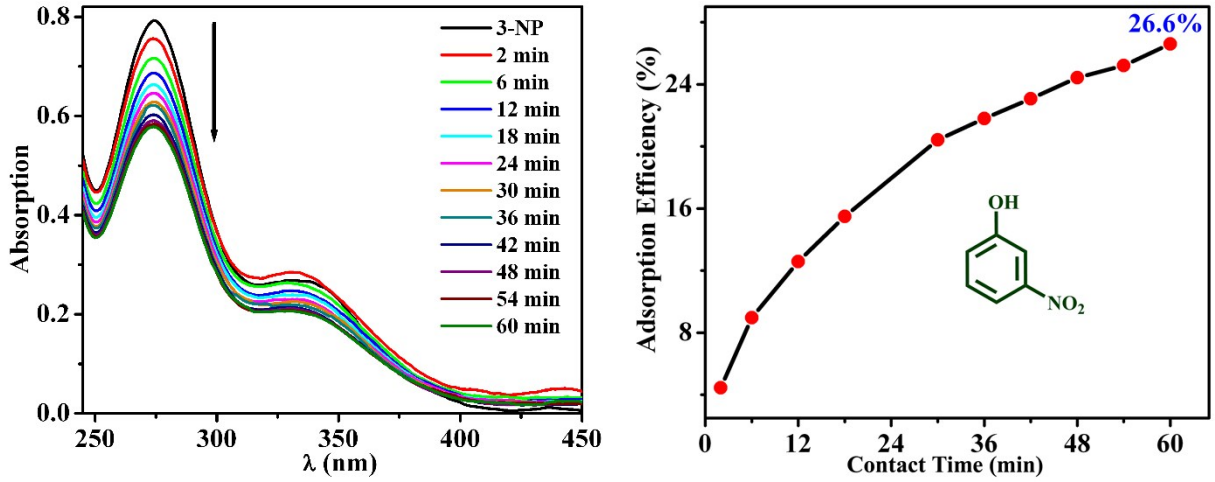

Fig. S17. Change in the absorption spectra of the water solution of 3-NP (0.5 mM) in the presence of **TB-COP** (3 mg) monitored at different time intervals (0→60 minutes) at 298 K and its corresponding adsorption efficiency plot (right).

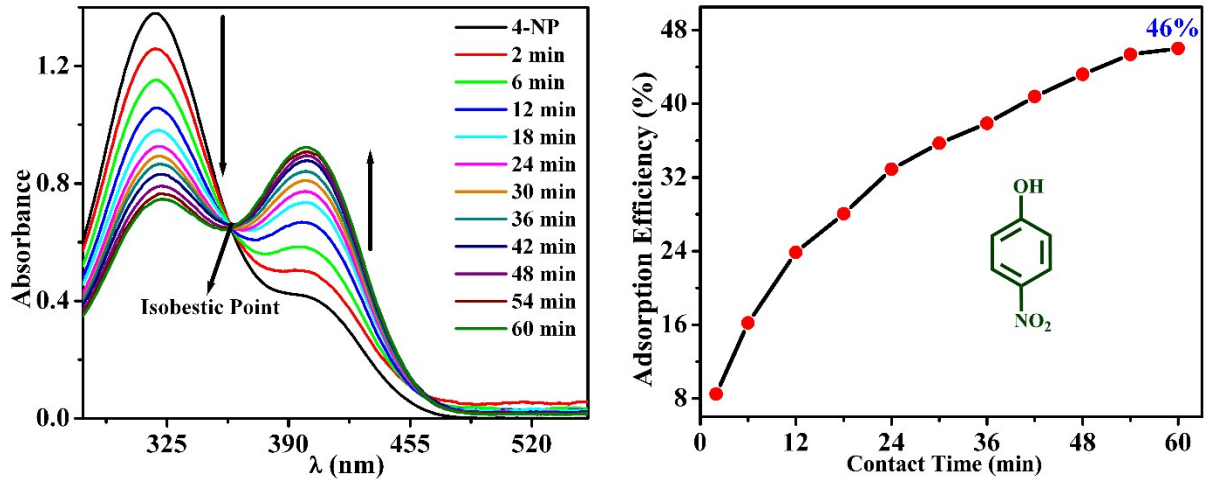

Fig. S18. Change in the absorption spectra of the water solution of 4-NP (0.5 mM) in the presence of **TB-COP** (3 mg) monitored at different time intervals (0→60 minutes) at 298 K and its corresponding adsorption efficiency plot (right).

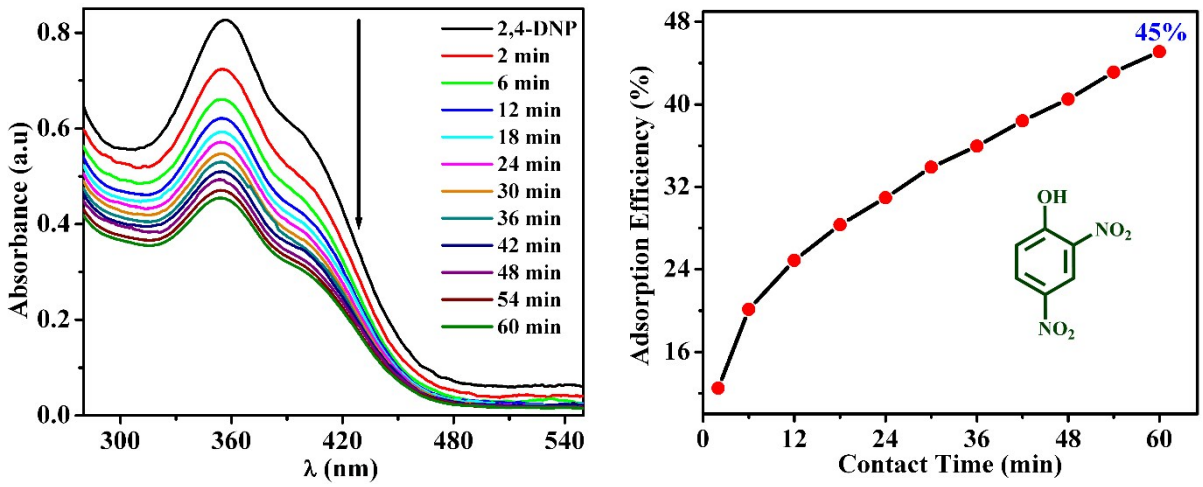

Fig. S19. Change in the absorption spectra of the water solution of 2,4-DNP (0.5 mM) in the presence of **TB-COP** (3 mg) monitored at different time intervals (0→60 minutes) at 298 K and its corresponding adsorption efficiency plot (right).

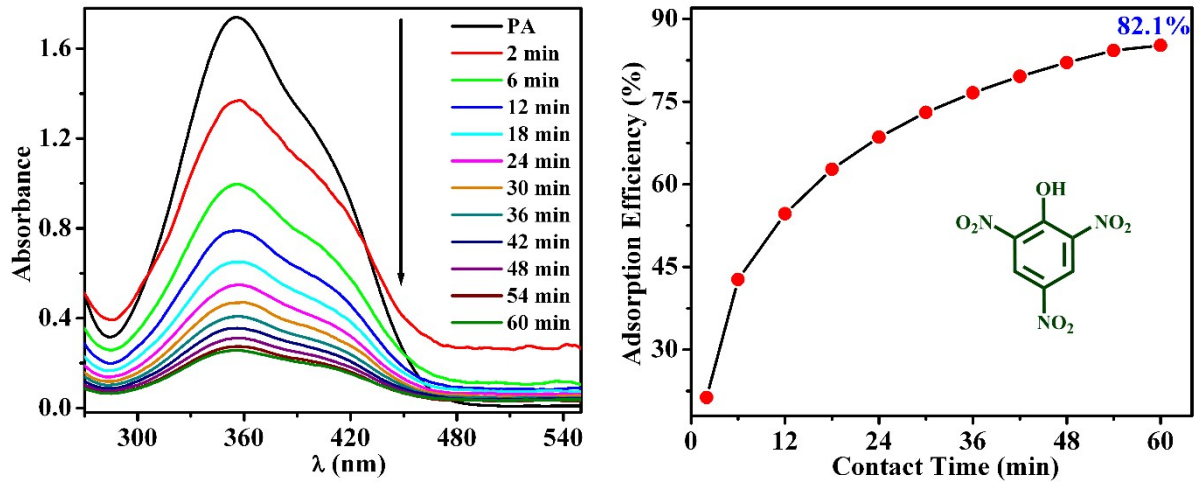

Fig. S20. Change in the absorption spectra of tap water solution of PA (0.5 mM) in the presence of **TB-COP** (3 mg) monitored at different time intervals (0→60 minutes) at 298 K and its corresponding adsorption efficiency plot (right).

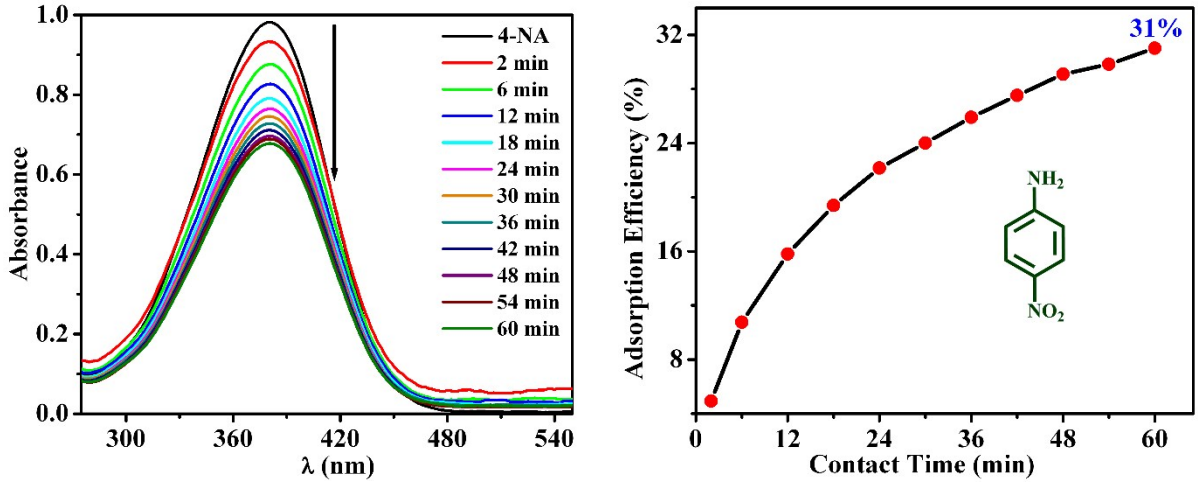

Fig. S21. Change in the absorption spectra of the water solution of 4-NA (0.5 mM) in the presence of **TB-COP** (3 mg) monitored at different time intervals (0→60 minutes) at 298 K and its corresponding adsorption efficiency plot (right).

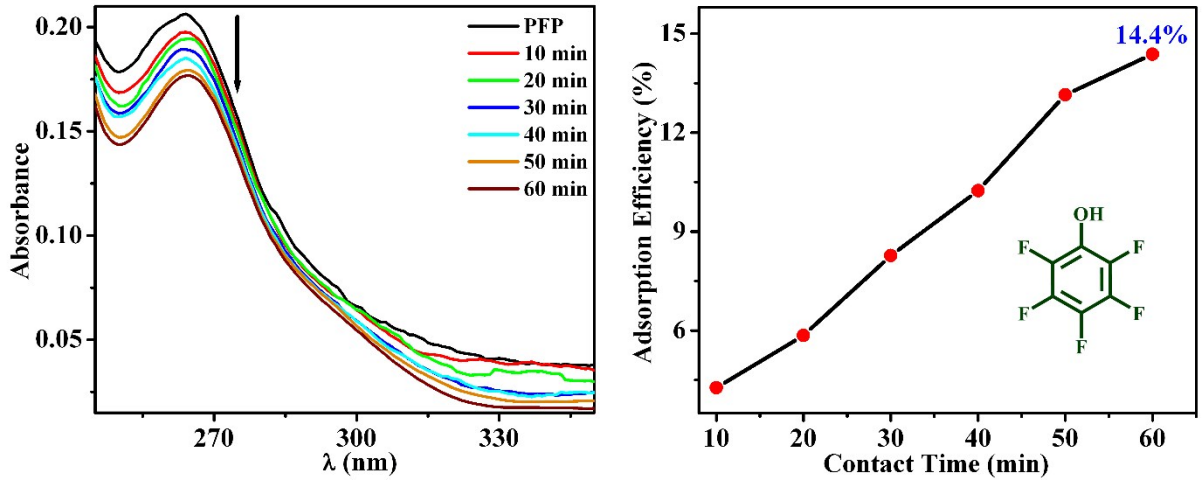

Fig. S22. Change in the absorption spectra of the water solution of PFP (0.5 mM) in the presence of **TB-COP** (3 mg) monitored at different time intervals (0→60 minutes) at 298 K and its corresponding adsorption efficiency plot (right).

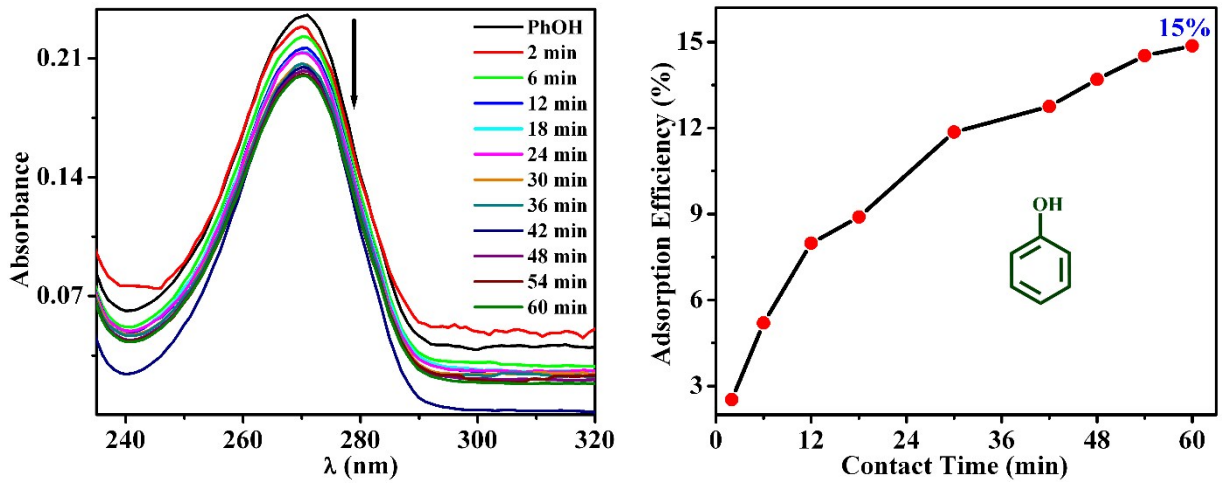

Fig. S23. Change in the absorption spectra of the water solution of PhOH (0.5 mM) in the presence of **TB-COP** (3 mg) monitored at different time intervals (0→60 minutes) at 298 K and its corresponding adsorption efficiency plot (right).

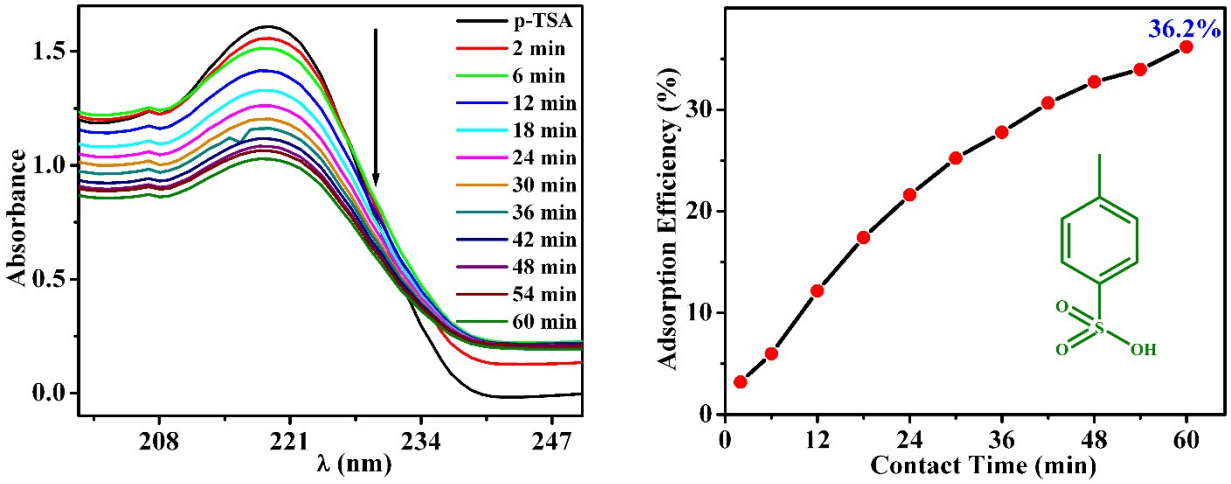

Fig. S24. Change in the absorption spectra of the water solution of p-TSA (0.5 mM) in the presence of **TB-COP** (3 mg) monitored at different time intervals (0→60 minutes) at 298 K and its corresponding adsorption efficiency plot (right).

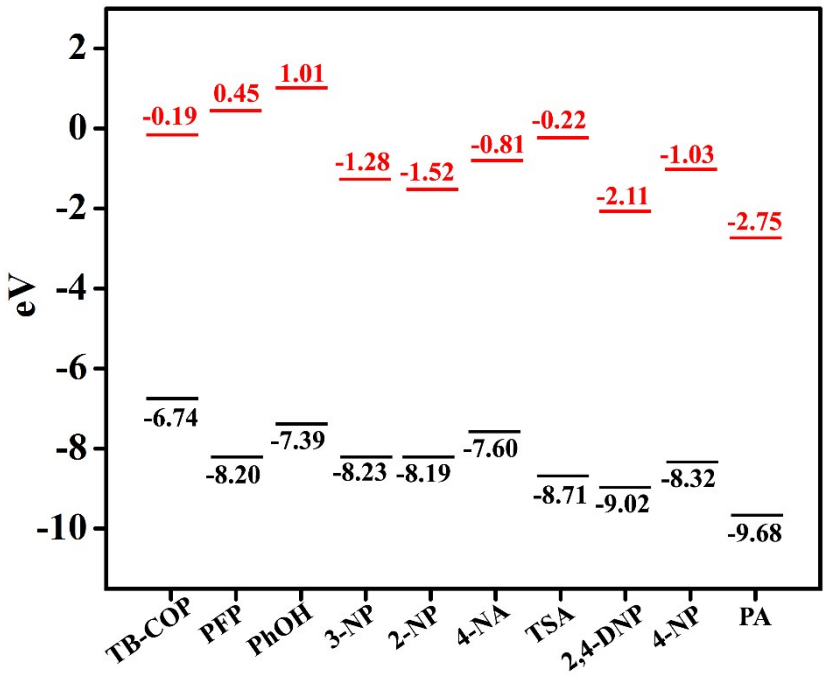

Fig. S25. HOMO and LUMO energies for selected analytes and the **TB-COP** adsorbent.

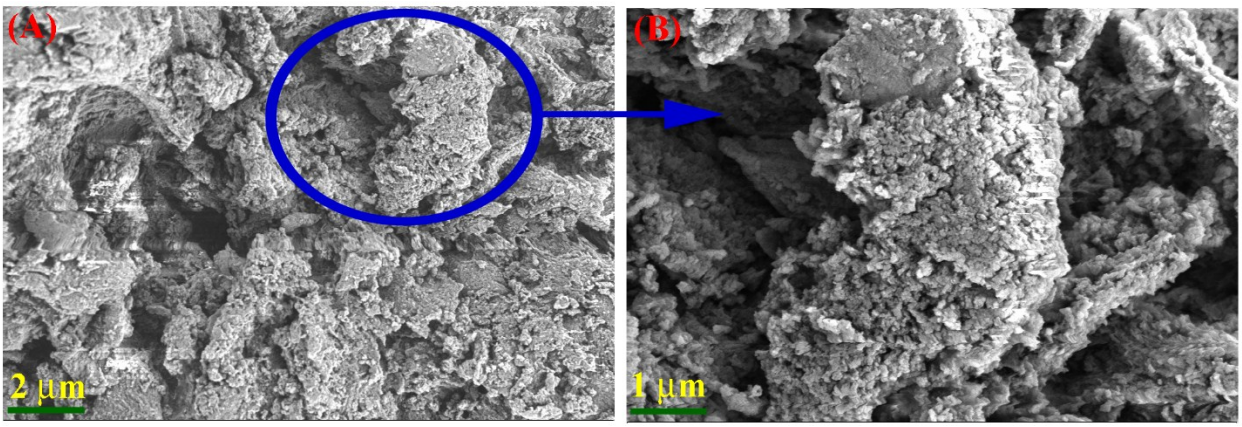

Fig. S26. Scanning electron microscopy image (A) and its enlarged image (B) of recycled **TB-COP** after 5th cycle.